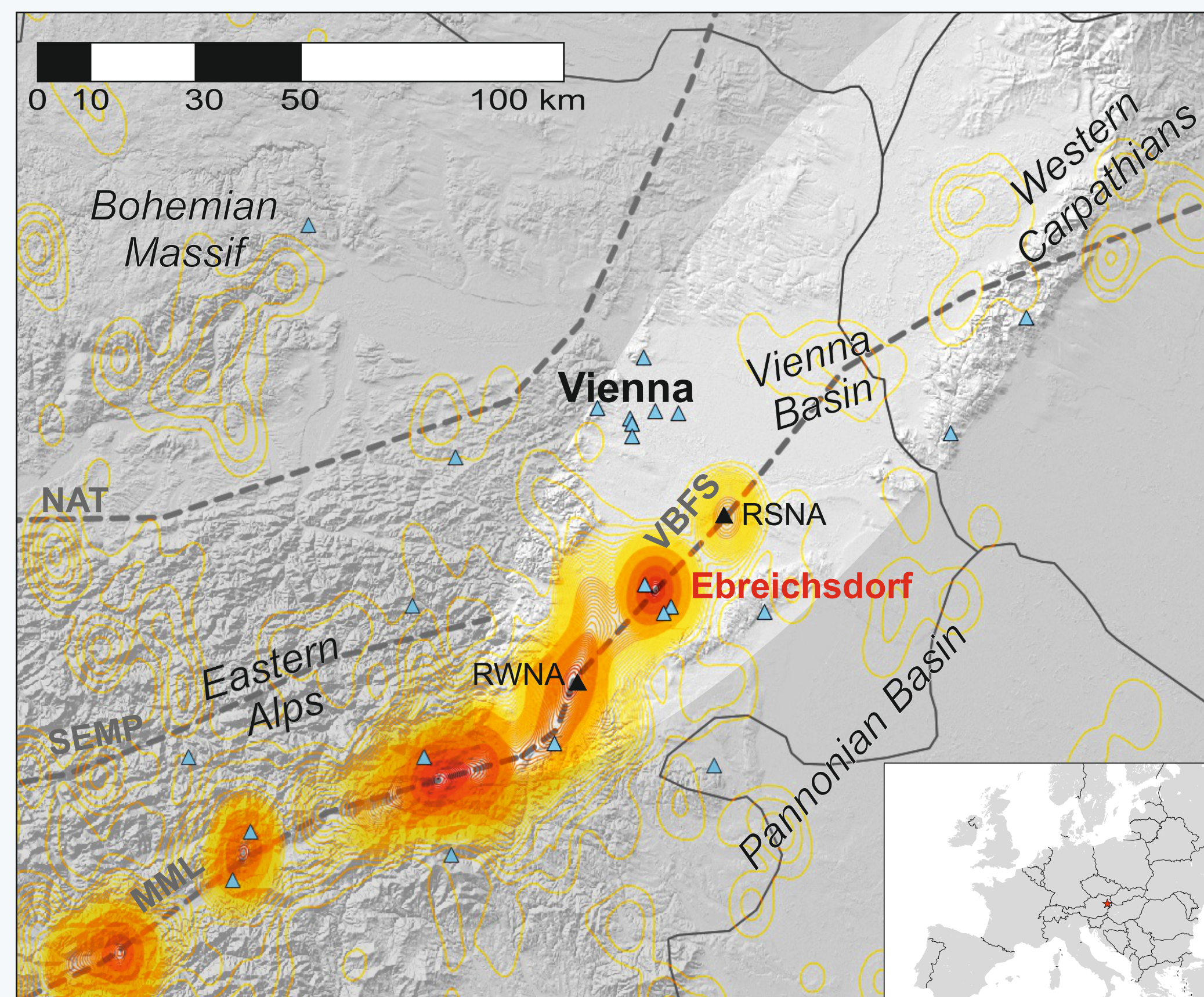


Abstract

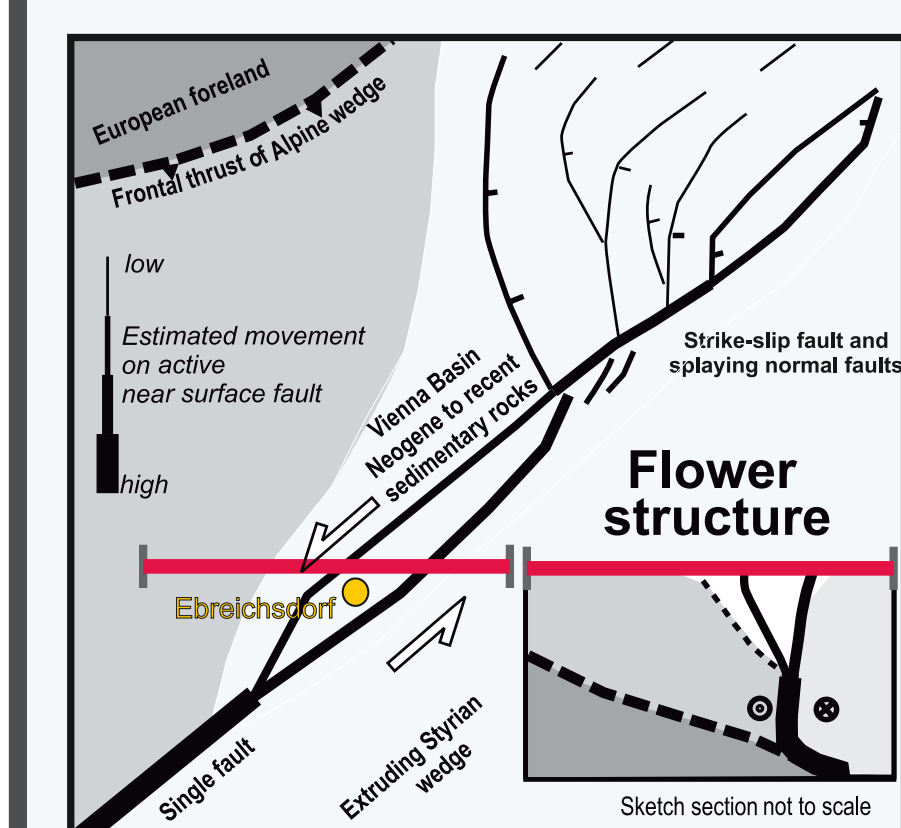
Eastern Austria is a region of low to moderate seismicity, and hence the seismological network coverage is relatively sparse. Nevertheless, the area is one of the most densely populated and most developed areas in Austria, in particular Vienna and its surroundings. The largest instrumentally recorded magnitude is around 5, and the Vienna Basin Fault System (VBFS) occasionally shows earthquakes with magnitudes larger than 4. The background seismicity along the VBFS seems to occur in discrete clusters. One of them is located near Ebreichsdorf. In this area, two pairs of events followed by a few tens of aftershocks happened at a 13 year interval. The earthquake cluster in 2013 including 2 main shocks ($M_1 \sim 4.2$) as well as almost 30 aftershocks was recorded with a multitude of close-by seismic stations. In this study, we relocate these events with hypoDD 3D with all to us available stations in a range of 240 km. Afterwards, we locate the two main shocks from a similar swarm in 2000, relative to the main shocks in 2013. Moreover, we investigate possible interactions between the 2013 earthquakes with moment magnitudes ~ 4.5 . We analyse the data with the objectives of revealing the conditions behind their occurrences and help assess the seismic hazard in the region.

Tectonic setting and regional seismicity



Due to ongoing convergence between the European Plate from the north and the Adriatic plate from the south, crustal blocks laterally extrude to the east into the Pannonian Basin (e.g., Brückl et al. (2010)). Two sinistral strike-slip faults show this process: the Salzach-Enns-Mariazell-Puchberg (SEMP) and the more seismically active Mur-Mürz-Linie (MML). The Vienna Basin lies in the north-western extension of those faults, in the transition of the Eastern Alps to the Western Carpathians. This pull-apart basin that started forming in the Early Miocene, is now filled with sediment layers of a few kilometers. Here, the SEMP and the MML migrate into the Vienna-Basin-Fault-System (VBFS). Under the sediment layers the Bohemian Massif forms the underground of the Vienna Basin, at depths between 3 and 8 km (Wessely, 1983). An overview of the main tectonic units, faults and seismicity is given in the figure above.

Simplified tectonic structure



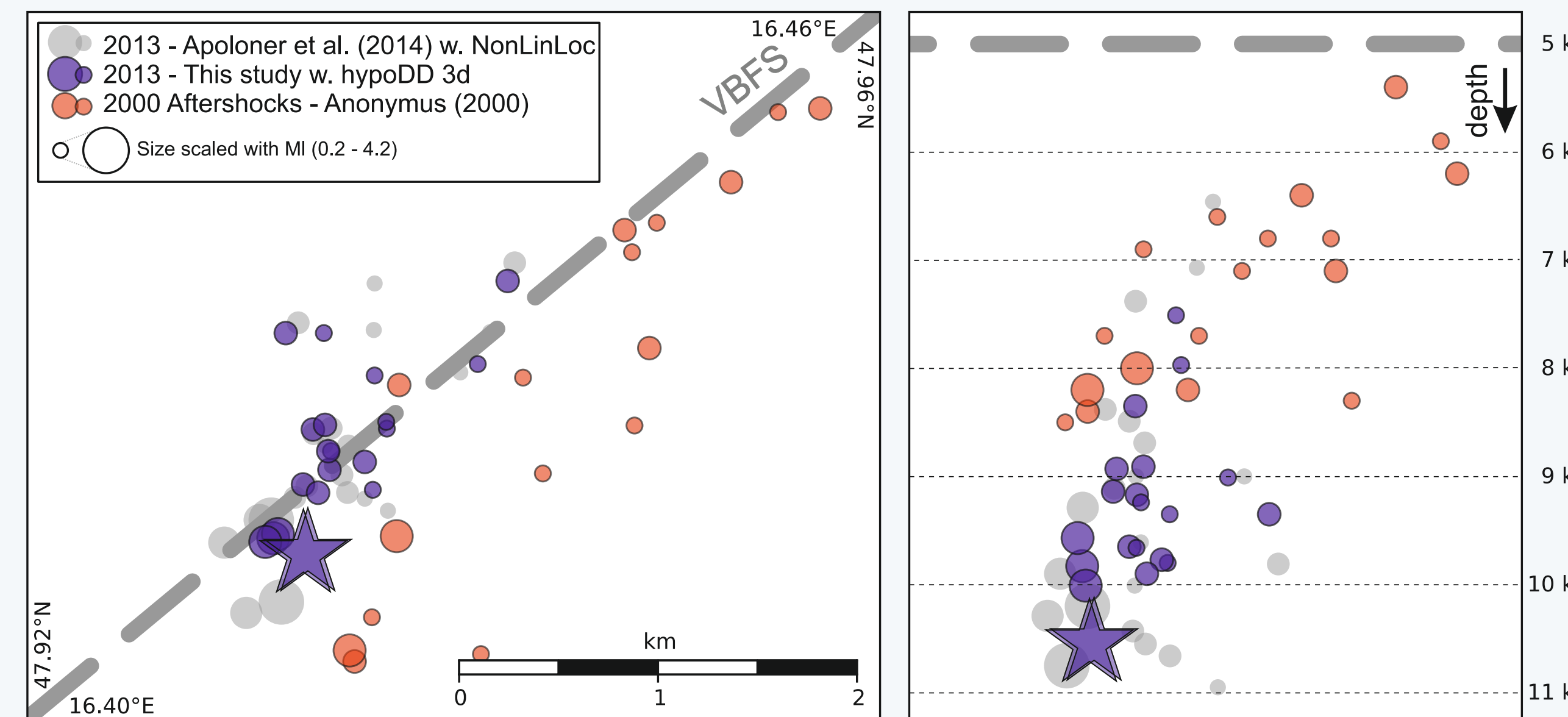
The Ebreichsdorf area is located in the continuation of the MML fault zone as the pull-apart system of the Vienna basin is opening toward the North-East. Seismic imaging shows that, around this location, the VBFS change from a single sinistral fault to a negative flower structure forming a small-scale basin approximately 4-6 km deep (Hinsch et al., 2005). The deeper structure of the VBFS is uncertain. The negative flower structure seems to merge into a single plane, which may perhaps merges with the main detachment of the Vienna pull-apart basin. The figure on the left shows the schematic tectonic structure of the small scale pull-apart basin around Ebreichsdorf (Modified from Hinsch et al. (2005)).

References

Anonymus. Investigation of the aftershocks of the earthquake of Ebreichsdorf from 11th July, 2000 near Vienna. Report of the on site inspection group of the ctbto, Comprehensive Test Bed Treaty Organization, CTBO, Vienna, Austria, 2002.
 M.-T. Apoloner, G. Bokelmann, I. Bianchi, E. Brückl, H. Hausmann, S. Merli, and R. Meurers. The 2013 earthquake series in the southern Vienna basin: location. *Advances in Geosciences*, 36:77-80, 2014. doi: 10.5194/adgeo-36-77-2014. URL: http://www.adgeo-advances.com/36/77/2014/.
 N. M. Beeler, R. W. Simpson, S. H. Hickman, and D. A. Lockner. Pore fluid pressure, apparent friction, and Coulomb failure. *Journal of Geophysical Research: Solid Earth*, 105(B11):25533-25542, 2000. ISSN 2155-2202. doi: 10.1029/2000JB001101. URL: http://dx.doi.org/10.1029/2000JB001101.
 M. Behm, E. Brückl, W. Chvalat, and H. Thybo. Application of stacking and inversion techniques to three-dimensional wide-angle reflection and refraction seismic data of the eastern alps. *Geophysical Journal International*, 170:275-298, 2007a.
 M. Behm, E. Brückl, and U. Mitterbauer. A new tectonic model of the eastern alps and its relevance for geodesy and geodynamics. *VGI Österreichische Zeitschrift für Vermessung & Geoinformation*, 2:121-133, 2007b.
 M. Beyreuther, R. Barsch, L. Krischer, T. Meigs, Y. Behr, and F. Wassermann. Obspy: A python toolbox for seismology. *Seismological Research Letters*, 81(3):530-533, 2010.
 E. Brückl, M. Behm, K. Decker, M. Grad, A. Guterch, C. R. Keller, and H. Thybo. Crustal structure and active tectonics in the eastern alps. *Tectonics*, 29(2), 2010. ISSN 1944-9794. doi: 10.1029/2009TC003991. URL: http://dx.doi.org/10.1029/2009TC003991.
 E. Brückl, R. Weber, M.T. Apoloner, J. Brückl, and W. Loder. J. Maras, S. Merli, G. Moeller, B. Schurr, S. Weginger, and E. Ummig. Seismological and geodetic monitoring of alpine/pannonian active tectonics - final report. Technical report, Österreichische Akademie der Wissenschaften, Vienna, Austria, 2014.
 R. Hinsch, K. Decker, and M. Wagsrieh. 3-d mapping of segmented active faults in the southern Vienna basin. *Quaternary Science Reviews*, 24(3-4):321-336, 2 2005. doi: http://dx.doi.org/10.1016/j.quascirev.2004.04.011. URL: http://www.sciencedirect.com/science/article/pii/S0273791944061994.
 A. Jarvis, H. Reuter, A. Nelson, and E. Guevara. Hole-filled seamless srtm data v4, 2008. URL: http://srtm.csi.cgiar.org.
 G. C. P. King, R. S. Stein, and J. Lin. Static stress changes and the triggering of earthquakes. *Bulletin of the Seismological Society of America*, 84(3):935-953, 06 1994.
 W. Lenhardt, Ch. Freudenthaler, R. Lippitsch, and E. Flegewell. Focal-depth distributions in the austrian eastern alps based on macroseismic data. *Austrian Journal of Earth Sciences*, 100:66-79, 2007.
 J. Lin and R. S. Stein. Stress triggering in thrust and subduction earthquakes and stress interaction between the southern san andreas and nearby thrust and strike-slip faults. *Journal of Geophysical Research: Solid Earth*, 109(B2), 2004. ISSN 2155-2202. doi: 10.1029/2003JB002067. URL: http://dx.doi.org/10.1029/2003JB002067.
 A. Lomax, J. Virieux, P. Volant, and C. Berge. Advances in seismic event locations, chapter Probabilistic earthquake location in 3D and layered models: Introduction of a Metropolis-Gibbs method and comparison with linear locations, pages 101-134. Kluwer, Amsterdam, 2000.
 SED. Reviewed regional moment tensor catalog. ONLINE, April 2006. URL: http://www.seisao.ethz.ch/prod/tensors/rt_olocat.
 R. S. Stein, A. A. Barka, and J. H. Dieterich. Progressive failure on the north anatolian fault since 1939 by earthquake stress triggering. *Geophysical Journal International*, 132(3):594-604, 1997. doi: 10.1111/j.1365-246X.1997.tb05311.x. URL: http://gji.oxfordjournals.org/content/132/3/594.abstract.
 S. Toda, R. S. Stein, K. Richards-Dinger, and S. B. Bockert. Forecasting the evolution of seismicity in southern california: Animations built on earthquake stress transfer. *Journal of Geophysical Research: Solid Earth*, 110(B5), 2005. ISSN 2155-2202. doi: 10.1029/2004JB003415. URL: http://dx.doi.org/10.1029/2004JB003415.
 G. Wessely. Zur geologie und hydrodynamik im südlichen wiener becken und seiner randzone. *Mit. oester. geol. Gesellschaft*, 76:27-68, 1983.
 ZAMG. Austrian earthquake catalogue of earthquakes from 1200 to 2013 a.d. (austrian). computer file of earthquakes with ml and defining picks >= 6. E. Central Institute of Meteorology and Geodynamics (ZAMG), 2014.

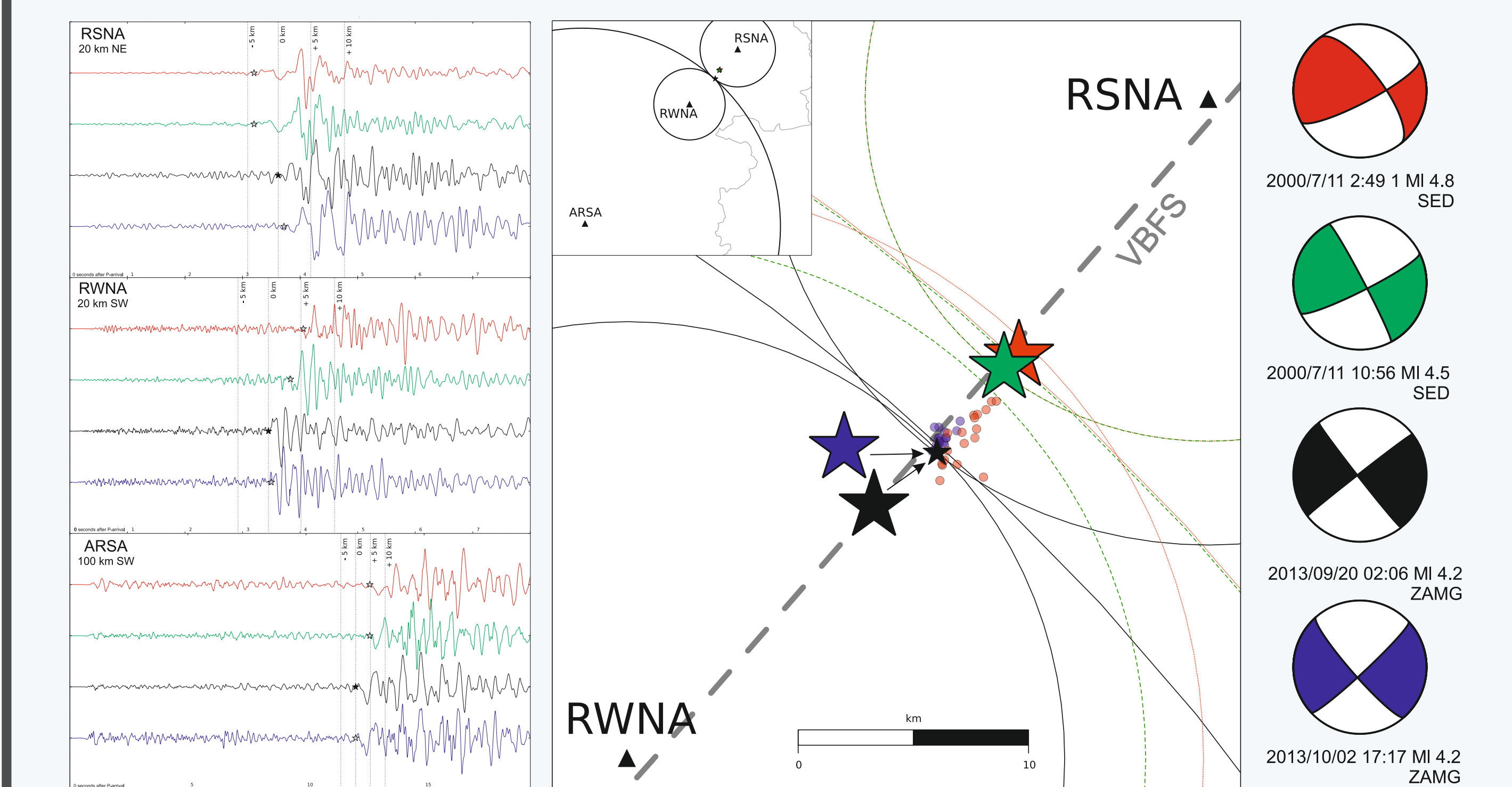
Hypocenter location with hypoDD 3D

Usually earthquake location and depth estimation in this area is difficult because the closest seismic station is 40 km away. As part of a project by the Technical University of Vienna 10 seismic stations were deployed in the Vienna Basin (see Brückl et al. (2014) for details). The University of Vienna deployed three additional stations close to the epicenter of the aftershocks. Apoloner et al. (2014) located the swarm using the data from all available seismic stations using NonLinLoc by Lomax et al. (2000) and the 3D-P- and S-wave models by Behm et al. (2007b) and Behm et al. (2007a). These locations entered as initial locations into hypoDD 3D by Waldhauser (personal communication Feb. 2014). We adapted the same 3D-model. Cross-correlation with values up to 0.7 complete the dataset.



After relocation the cluster scatters less, as can be seen in the figure above. In particular the two main shocks are now less than 40 m apart. There is a clear trend in event depth with smaller events being shallower than bigger events. However, even with relative locations, no distinct event pattern in time is apparent. The mean hypocentral depth is around 9.5 km, which is typical in this region as described e.g. Lenhardt et al. (2007). We conclude that the hypocenters are beneath the principal displacement zone of the flower structure that is assumed for this area. Furthermore, the epicenters show a South-West to North-East pattern, which allocates them to the Vienna Basin Fault System.

Location of 2000 and 2013 main shocks



Only three stations at a distance of less than 100 km recorded the main shocks in 2000 and 2013. We compared the S-P-difference-times for those 4 events, and located them relative to the event from the 2013/09/20. The figure above shows that both events from 2013 are close together, whereas the difference in S-P-times moves the events 5 km to the North-East.

Coulomb stress change

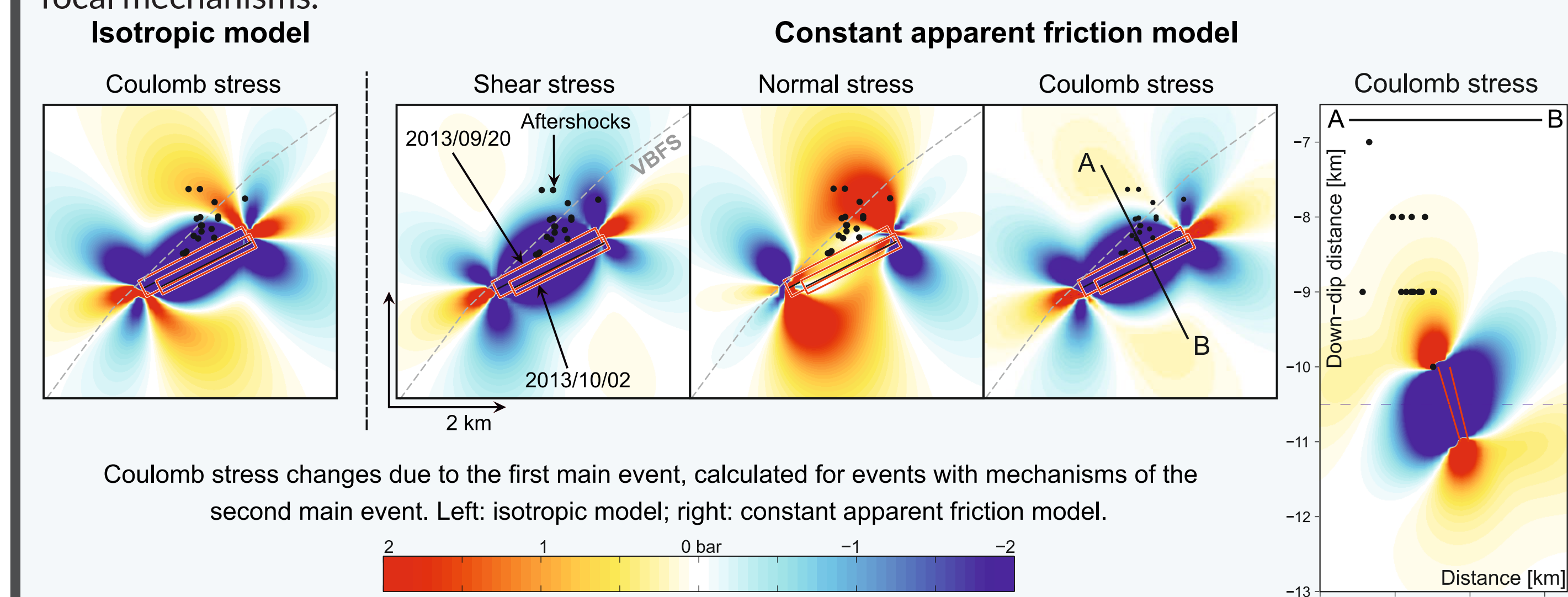
The triggering of earthquakes and/or aftershocks is often explained by static stress transfer between events (e.g. King et al. (1994); Stein et al. (1997)). The Coulomb failure criterion is generally used to quantify the static stress perturbation due to an earthquake. **Coulomb-Mohr failure:** The Coulomb-Mohr failure criterion is an experimental relation describing frictional sliding and failure of rocks. Incorporating the principle of effective stress of Terzaghi, and for the change of Coulomb stress (static perturbations) after an earthquake, the Coulomb criterion becomes (Beeler et al., 2000):

$$\Delta\sigma_c = \Delta\tau_r - \mu(\Delta\sigma_n - \Delta p)$$

with $\Delta\tau_r$ the change in shear stress in the slip direction, μ the coefficient of internal friction, $\Delta\sigma_n$ the change in fault-normal stress, and Δp the change in pore pressure. Positive changes bring closer to failure and vice-versa for negative changes. Two models are generally in use, depending on how pore pressure is included in the Coulomb criterion. In the apparent friction model, the mean stress $\Delta\sigma_m$ is assumed to be equal to the fault-normal stress and the apparent friction coefficient is then $\mu' = \mu(1 - B)$, with B the Skempton coefficient. Using the isotropic poroelastic model, for a homogeneous medium in undrained conditions, changes in pore pressure are related to the mean stress as: $\Delta p = B\Delta\sigma_m/3$.

Earthquake interactions of 2013 main shocks

Model parameters: The Coulomb stress perturbation are calculated with the Coulomb 3.3 software (Toda et al. (2005); Lin and Stein (2004)) using the apparent friction and the isotropic models. The main parameters used are an apparent friction coefficient μ' of 0.35, corresponding to a coefficient of friction μ of 0.7 and a Skempton coefficient of 0.5, a Young modulus of $7.5 \cdot 10^5$ bars, and a Poisson ratio of 0.25. The fault parameters are derived from their magnitudes and scaling relationships. They are between 1-2 km long, 1 km wide, and with an average displacement of a few centimeters, corresponding to a moment magnitude of ~ 4 . The stress perturbations are calculated for the first main event, assuming receiver faults with the geometry of the second main event. Calculation using receiver faults with the geometry of the first event gives similar results as both main events have similar focal mechanisms.



Results and interpretation: Considering shear and Coulomb stresses, the second main event is located in the shadow of the first event. It is, however, partially in the zone of the normal stress increase (unclamping). If the first event caused the second one, then the response from the disturbance coming from the first main event would have been delayed by ~ 12 days. This would imply some in situ relaxation mechanism, potentially involving fluid diffusion in the surroundings of the first main event, as both events are located very close to each other. The aftershocks are located above the two main shocks, in areas of positive Coulomb stress changes (due to shear stress increase). These events seem to delineate a plane above the two main shocks which follows the presumed trace of the Vienna Basin Fault System in this area. In our case, the results from the isotropic model are relatively similar to those of the apparent friction model.

Further research

Future analysis can include aftershocks occurring directly after the main shocks, as well as stress perturbations due to the second main shock. Also, the events from 2000 could be analysed. The dataset can also be used to try deduce methods usable for other events in the area and as a starting point for better delineation of the VBFS.

Acknowledgments

We would like to thank ZAMG, TU, ORFEUS and GeoRisk Earthquake Engineering for making available seismic data for this study. Topographic data used in maps was taken from SRTM (Jarvis et al., 2008) and historic seismicity from the Austrian Earthquake Catalog before 2013 (ZAMG, 2014). Plots were created with ObsPy (Beyreuther et al., 2010). Focal mechanisms are from SED (2006) and Freudenthaler-Pascher, ZAMG (personal communication, June 2014). Aftershock locations for 2000 are taken from Anonymus (2002)